Short Article

Cell Metabolism

Pharmacologic Effects of FGF21 Are Independent of the "Browning" of White Adipose Tissue

Graphical Abstract

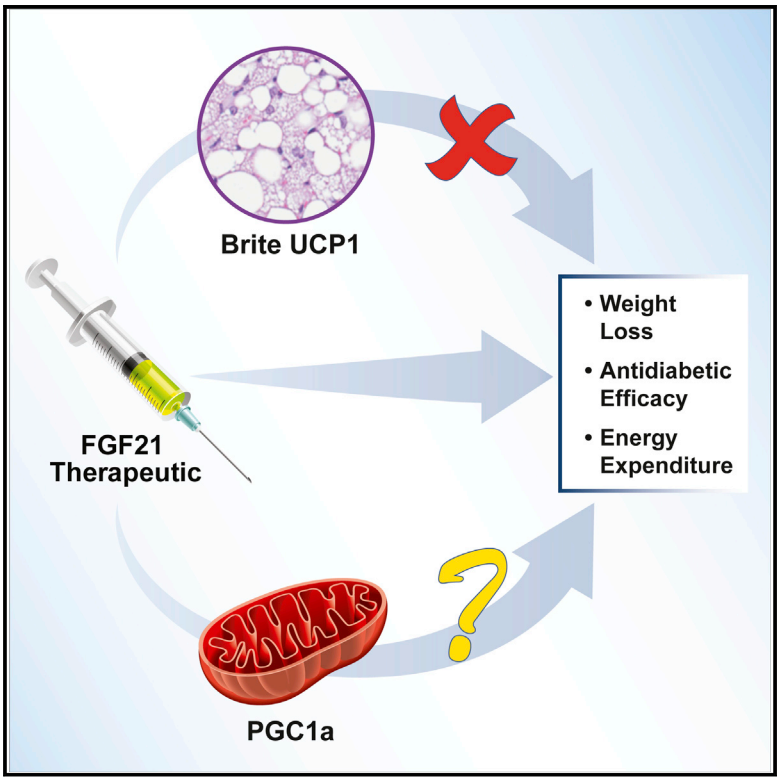

Authors

Murielle M. Véniant, Glenn Sivits, ..., Carolyn Moyer, David J. Lloyd

Correspondence

dlloyd@amgen.com

In Brief

Part of the beneficial pharmacological effects of FGF21 therapy is ascribed to "browning" of white adipose tissue. Véniant et al. show here that FGF21-induced browning is temperature dependent and that the effects on body weight reduction and glucose homeostasis can occur in UCP1 KO mice

Highlights

- The browning of white adipose tissue by FGF21 is temperature and diet dependent
- FGF21's antidiabetic and antiobesogenic effects are independent of brite adipocytes
- FGF21 is efficacious in *Ucp1* null mice

Véniant et al., 2015, Cell Metabolism *21*, 731–738
May 5, 2015 ©2015 Elsevier Inc.
http://dx.doi.org/10.1016/j.cmet.2015.04.019

Cell Metabolism
Short Article

Pharmacologic Effects of FGF21 Are Independent of the "Browning" of White Adipose Tissue

Murielle M. Véniant,[1] Glenn Sivits,[1] Joan Helmering,[1] Renee Komorowski,[1] Jae Lee,[1] Wei Fan,[1] Carolyn Moyer,[2] and David J. Lloyd[1,*]
[1]Department of Metabolic Disorders
[2]Department of Pathology
Amgen Inc., One Amgen Center Drive, Thousand Oaks, CA 91320, USA
*Correspondence: dlloyd@amgen.com
http://dx.doi.org/10.1016/j.cmet.2015.04.019

SUMMARY

"Browning," the appearance and activation of brown-in-white (brite) adipose cells within inguinal white adipose tissue (iWAT), and induction of uncoupling protein 1 (UCP1) correlate with fibroblast growth factor-21 (FGF21)-induced weight loss and glucose homeostasis improvements. Therefore, anti-obesity therapies targeting browning and brite adipocyte activation are currently being sought. To test the dependence of weight loss on browning, we examined whether this event was responsible for FGF21-Fc's beneficial effects. Lean and diet-induced obese mice housed at 21°C or 30°C that received FGF21-Fc exhibited similar degrees of body weight reduction and glucose homeostasis improvement. Substantial browning of iWAT occurred only in FGF21-Fc-treated lean mice housed at 21°C. Further, FGF21-Fc-treated *Ucp1*$^{-/-}$ mice showed robust improvements in body weight, glucose homeostasis, and plasma lipids, associated with increased energy expenditure and FGF21-Fc-induced *Ppargc1* expression in iWAT. We conclude that FGF21 requires neither UCP1 nor brite adipocytes to elicit weight loss and improve glucose homeostasis.

INTRODUCTION

In mammals, brown adipose tissue (BAT) preserves body temperature through nonshivering thermogenesis enabled by release of intracellular BAT lipids during lipolysis and heat generation in mitochondria via uncoupling protein 1 (UCP1) (Chechi et al., 2013). There are two types of BAT: classic BAT is derived from myogenic factor 5 (*myf5*), a muscle-like cell lineage, predominantly populating interscapular and subcutaneous regions in rodents and humans; adaptive BAT (beige or brown-in-white [brite]) is characterized by a non-*myf5*-derived lineage expressing UCP1 (Giralt and Villarroya, 2013). Brite adipocytes are multilocular lipid-containing cells located in inguinal white adipose tissue (iWAT; Emanuelli et al., 2014). Cold exposure markedly induces classic BAT and brite adipocytes (Fisher et al., 2012) and correlates with the appearance of UCP1-positive cells in iWAT. Further, mitochondria from cold-adapted iWAT are functionally thermogenic (Shabalina et al., 2013) and dependent on UCP1 presence (Nedergaard et al., 2001).

Fibroblast growth factor-21 (FGF21) is an important metabolic regulator (Berglund et al., 2009; Coskun et al., 2008; Kharitonenkov et al., 2005; Xu et al., 2009) that profoundly induces UCP1 expression in BAT and iWAT (Adams et al., 2012; Emanuelli et al., 2014; Fisher et al., 2012; Hondares et al., 2010; Lee et al., 2014a). FGF21 signals via FGF receptor 1c and a coreceptor β-klotho (Foltz et al., 2012) expressed in BAT and iWAT (Ito et al., 2000). FGF21 is induced and secreted by rodent and human BAT upon thermogenic stimulation (Fisher et al., 2012; Hondares et al., 2011, 2014; Lee et al., 2014b; Sharp et al., 2012). It leads to iWAT browning and brite adipocyte appearance (Fisher et al., 2012), suggesting a critical role of brite adipocytes and UCP1 in eliciting its pharmacologic effect. FGF21 signaling in WAT is required for improvement of metabolic parameters such as body weight, glucose homeostasis, and plasma triglycerides (Véniant et al., 2012; Wu et al., 2011). The preservation of FGF21's metabolic effects in mice without interscapular BAT implicates iWAT brite adipocytes in FGF21-mediated antiobesogenic and antidiabetic actions (Emanuelli et al., 2014).

Although the primary role of BAT is thermogenesis, the outcome is an increase in energy expenditure. Pharmacologic BAT activation and metabolic inefficiency could improve conditions such as obesity; indeed, much research is now directed toward this area (Chechi et al., 2014; Sammons and Price, 2014). FGF21 has become a paradigm for UCP1 activation and brite adipocyte induction as a therapeutic strategy for obesity and diabetes. Given this growing interest, we examined the importance of brite adipocytes as antiobesity agents by evaluating their requirement for eliciting FGF21-induced weight loss and antidiabetic effects.

RESULTS AND DISCUSSION

FGF21-Fc Is Efficacious in Lean and Diet-Induced Obese Mice Housed in a Thermoneutral Environment

Thermoneutral zone (TNZ) housing (30°C) suppresses sympathetic tone and BAT-induced thermogenesis in mice, whereas industry-standard housing (21°C) activates BAT and brite adipose. Housing temperature can alter the effect of BAT-related factors such as bone morphogenetic protein 7 (Boon et al., 2013). To

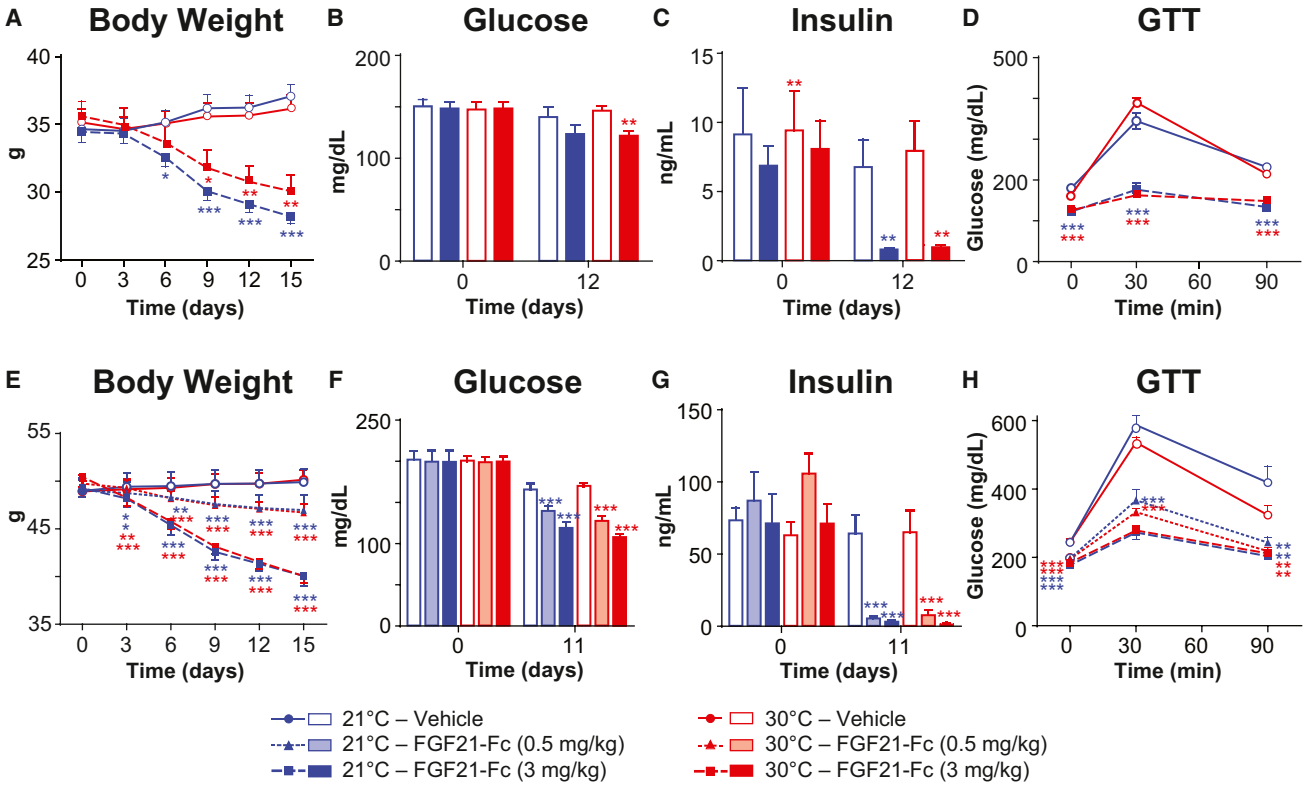

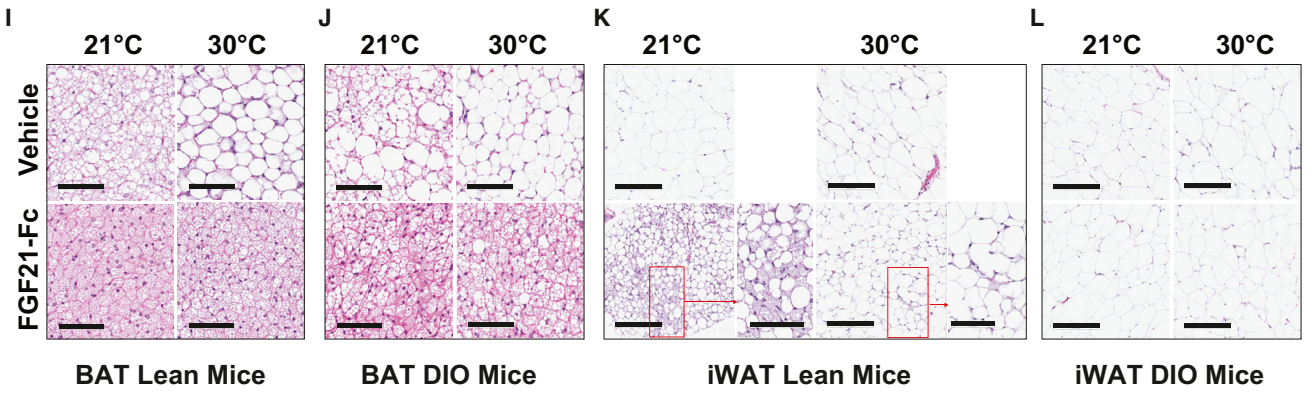

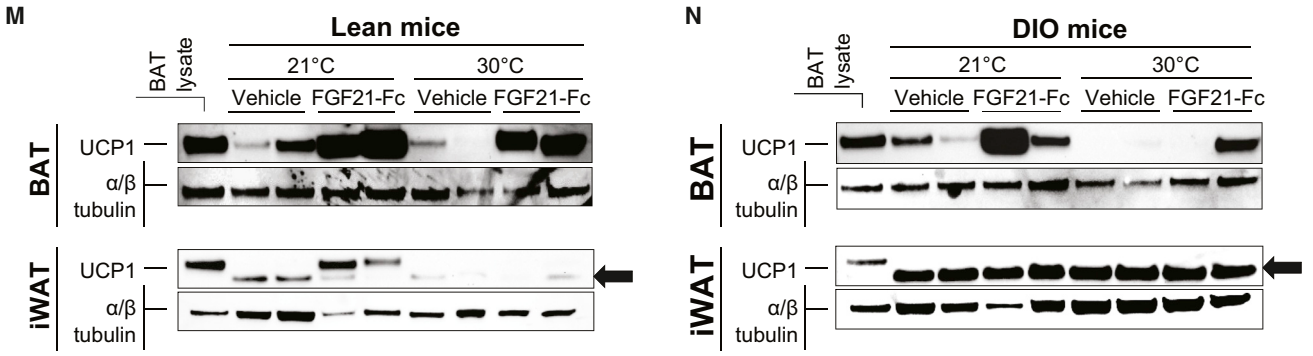

(legend on next page)

study the dependence of FGF21's effects on housing temperature and BAT/brite activity, we assessed two doses (submaximal and maximal) of a long-acting FGF21 analog, FGF21-Fc, in lean and diet-induced obese (DIO) mice housed in both environments (Figure 1). First we established and characterized treatment-naive lean and DIO mice at 21°C and 30°C (Animal Study Design I stage 1). Body weight, glucose tolerance, and insulin levels did not differ in both groups in either environment (see Table S1 available online), but BAT histology differed. BAT adipocytes were uniformly multilocular in lean mice at 21°C but primarily unilocular (>90%) in lean mice at 30°C (Figure S1). DIO mice at 21°C had equally distributed uni- and multilocular BAT adipocytes, whereas DIO mice at 30°C had primarily unilocular (>90%) BAT. iWAT adipocyte morphology did not differ between lean and DIO mice at either 21°C or 30°C.

After 15 days of FGF21-Fc treatment (Animal Study Design I stage 2), body weight, insulin/glucose levels, and glucose tolerance (hereafter termed beneficial effects) similarly improved in lean and DIO mice at 21°C or 30°C (Figures 1A–1H), and BAT adipocytes were uniformly multilocular (Figures 1I and 1J). In contrast, a temperature-dependent increase was seen in the number of individual and aggregates of multilocular brite adipocytes in iWAT of FGF21-Fc-treated lean mice. Most (seven of eight) of these mice housed at 21°C showed several variably sized brite adipocyte aggregates in iWAT, along with isolated cells (Figure 1K, inset; Table S2). Brite adipocyte appearance was substantially less at 30°C (Figure 1K). In contrast, iWAT of DIO mice at either 21°C or 30°C had microscopically identical isolated, rare (<1%), multilocular brite adipocytes with or without FGF21-Fc treatment (Figure 1L; Table S2). Thus, FGF21-Fc's beneficial effects occurred without multilocularity in iWAT, suggesting multilocular adipocyte activation in iWAT is of little significance in eliciting its beneficial effects.

To confirm the molecular extent of browning and multilocular cell appearance in iWAT of FGF21-Fc-treated mice, we assessed UCP1 protein induction in BAT and iWAT lysates from vehicle- and FGF21-Fc-treated lean and DIO mice housed in both environments. BAT of FGF21-Fc-treated lean (Figure 1M) and DIO (Figure 1N) mice at 21°C showed robust UCP1 expression; the induction was more modest at 30°C. In contrast, UCP1 induction by FGF21-Fc in iWAT was observed only in lean mice at 21°C (Figures 1M and 1N). UCP1 was below detection limit in iWAT of vehicle-treated lean mice and vehicle- and FGF21-Fc-treated DIO mice housed at both temperatures.

These data support our histologic findings that FGF21-Fc induces brite adipocytes and UCP1 in lean mice at 21°C but not in lean mice at 30°C or DIO mice at either temperature. Lack of detectable UCP1 induction in iWAT alongside FGF21-Fc's effects in these mice extends the finding that not only brite adipocyte expansion but also UCP1 expression can be dissociated from FGF21-Fc's beneficial effects.

FGF21-Fc Is Equally Beneficial in *Ucp1*$^{-/-}$ Mice

The link between FGF21-Fc's beneficial effects and UCP1 induction was further studied in *Ucp1*$^{-/-}$ mice. To relieve thermal stress, a colony of *Ucp1*$^{-/-}$ mice was raised at 30°C (Feldmann et al., 2009), which showed no overt phenotype differences versus control *Ucp1*$^{+/-}$ mice in these conditions (Table S3), consistent with previous reports (Enerbäck et al., 1997). *Ucp1*$^{+/-}$ and *Ucp1*$^{-/-}$ mice were treated with vehicle or FGF21-Fc for 17 days, and established endpoints (Xu et al., 2009) were assessed. Control mice had 18% lower body weight and 78% and 23% lower plasma insulin and glucose levels, respectively (Figures 2A–2C); glucose tolerance was improved (33% lower area under the curve [AUC]; Figure 2D). Given the increased UCP1 expression in iWAT of lean mice post-FGF21-Fc treatment (Figure 1M) (Fisher et al., 2012), we expected a diminished beneficial effect in FGF21-Fc-treated *Ucp1*$^{-/-}$ mice. Surprisingly, the beneficial effects in these mice were similar to those observed in *Ucp1*$^{+/-}$ mice: 14% lower body weight; ~70% and 6% lower plasma insulin and glucose levels, respectively; and 30% lower glucose tolerance AUC (Figures 2A–2D). Glucose level was not significantly reduced by FGF21-Fc in *Ucp1*$^{-/-}$ mice, but was significantly lower at glucose tolerance test (GTT; Figure 2D) initiation, confirming improved glucose homeostasis in these mice. Equal improvement in plasma lipids was seen in both mouse strains (Figures 2E–2G). UCP1 absence in iWAT and BAT of *Ucp1*$^{-/-}$ mice housed at 30°C was confirmed by immunoblot analysis (Figure 2H). UCP1 expression in BAT and iWAT of *Ucp1*$^{+/-}$ mice housed at 30°C was suppressed as brite adipocytes are not induced in TNZ environments. FGF21-Fc led to UCP1 induction in BAT of *Ucp1*$^{+/-}$ mice. As expected, UCP1 was absent in *Ucp1*$^{-/-}$ mice with or without exposure to FGF21-Fc, confirming the genotype of the mice. These data suggest that although FGF21-Fc influences UCP1 expression, energy dissipation via UCP1-mediated uncoupling does not account for its beneficial effect.

Figure 1. FGF21-Fc Is Efficacious in Lean and DIO Mice Housed in Standard or Thermoneutral Environments

(A–D) Chow-fed, lean mice housed at 21°C or 30°C were treated with vehicle or 3 mg/kg human FGF21-Fc per Animal Study Design I. Body weight was monitored over 15 days, plasma glucose and insulin levels were measured on days 0 and 12, and glucose tolerance was assessed on day 15.

(E–H) DIO mice housed at 21°C or 30°C were treated with 0.5 or 3 mg/kg human FGF21-Fc. Body weight was monitored over 15 days, plasma glucose and insulin levels were measured on days 0 and 11, and glucose tolerance was assessed on day 15.

(I) BAT morphology (H&E) of lean mice from (A)–(D). Bars represent 200 μm.

(J) BAT morphology (H&E) of DIO mice from (E)–(H). Bars represent 200 μm.

(K) iWAT morphology (H&E) of lean mice from (A)–(D). Bars represent 200 μm. Inset (red box) shows higher magnification of multilocular adipocytes. Bars represent 100 μm.

(L) iWAT morphology (H&E) of DIO mice from (E)–(H). Bars represent 200 μm.

(M and N) BAT and iWAT were excised from lean and DIO mice after completion of Animal Study Design I, and two lysates from each group were analyzed by immunoblot for UCP1. A BAT lysate from a wild-type C57BL/6 mouse was used as a positive control to highlight a nonspecific immunoreactive band in iWAT (arrow). α/β-tubulin was used as a loading control.

Data represent mean ± SEM (n = 8/group), analyzed by ANCOVA. *$p < 0.05$, **$p < 0.01$, ***$p < 0.001$ versus vehicle control. See also Figures S1 and S2 and Tables S1 and S2.

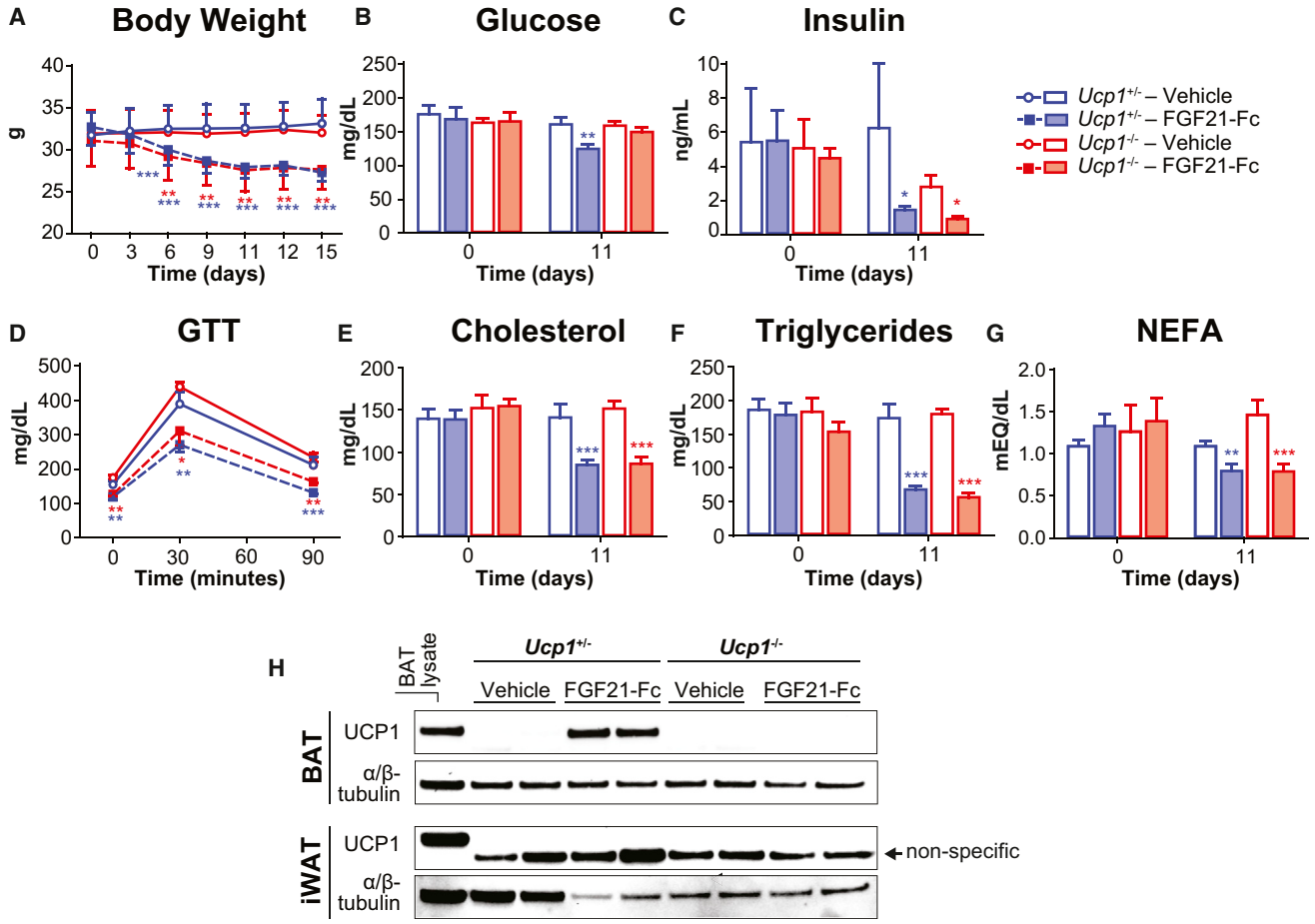

Figure 2. FGF21-Fc Is Efficacious in *Ucp1*$^{-/-}$ Mice

(A–G) *Ucp1*$^{+/-}$ and *Ucp1*$^{-/-}$ mice housed at 30°C were treated with vehicle or 3 mg/kg human FGF21-Fc as described in Animal Study Design II. Body weight was monitored over 15 days; plasma glucose, insulin, cholesterol, triglycerides, and NEFA were measured on days 0 and 11; and glucose tolerance was assessed on day 15. Data represent mean ± SEM (n = 4–6 mice/group), analyzed by ANCOVA. *p < 0.05, **p < 0.01, ***p < 0.001 versus vehicle control.

(H) Immunoblot analysis of BAT and iWAT lysates (two from each group) from *Ucp1*$^{+/-}$ and *Ucp1*$^{-/-}$ mice treated with human FGF21-Fc. A BAT lysate from a wild-type C57BL/6 mouse was used as a positive control to highlight a nonspecific band (arrow). α/β-tubulin was used as a loading control. See also Table S3.

FGF21-Fc Increases Energy Expenditure in *Ucp1*$^{-/-}$ Mice

FGF21 increases energy expenditure in DIO mice housed at 21°C (Xu et al., 2009). To explore the possible reason for FGF21-Fc's beneficial effects in *Ucp1*$^{-/-}$ mice, we conducted food intake and indirect calorimetry studies. First we established reproducibility of FGF21-Fc's effects on body weight in *Ucp1*$^{+/-}$ and *Ucp1*$^{-/-}$ mice (Figure 3A). Reduced food intake was not responsible for weight loss; in fact, when standardized to body weight, FGF21-Fc increased food intake in *Ucp1*$^{-/-}$ mice, with similar trends in *Ucp1*$^{+/-}$ mice (Figure 3B). In contrast, O_2 consumption and CO_2 production dramatically increased (Figures 3C and 3D). This effect was more significant in *Ucp1*$^{+/-}$ mice, indicating a slightly diminished FGF21-Fc effect in *Ucp1*$^{-/-}$ mice. Substrate oxidation preference, inferred from respiratory exchange ratio, was unchanged in all FGF21-Fc-treated mice (Figure 3E). FGF21-Fc did not alter physical activity in *Ucp1*$^{+/-}$ mice but mildly increased it in *Ucp1*$^{-/-}$ mice during the day (Figure 3F). These data support the fact that FGF21-Fc-induced weight loss is caused not by changes in food intake or specific increases in substrate utilization but by increases in energy expenditure in *Ucp1*$^{+/-}$ and *Ucp1*$^{-/-}$ mice.

FGF21-Fc-Induced Gene Expression Changes in *Ucp1*$^{+/-}$ and *Ucp1*$^{-/-}$ Mice

Although UCP1 is established as the predominant thermogenic protein (Nedergaard et al., 2001), we assayed possible compensation by UCP2/3 (Figure 4). First we observed that FGF21-Fc induced *Ucp1* expression in *Ucp1*$^{+/-}$ BAT and iWAT. Notably, this was not detected at the protein level in iWAT (Figure 2H), presumably owing to the higher sensitivity of the RT-PCR technique. *Ucp1* was undetectable in iWAT of vehicle-treated *Ucp1*$^{+/-}$ mice and prevented calculation of a fold change from vehicle- to FGF21-Fc-treated mice. As expected, *Ucp1* was undetectable in *Ucp1*$^{-/-}$ mice; however, an outlier was identified, highlighted, and excluded from statistical analyses. *Ucp2* expression in adipose tissue of *Ucp1*$^{+/-}$ and *Ucp1*$^{-/-}$ mice was mostly unaltered by FGF21-Fc, though reduced expression was observed in BAT of *Ucp1*$^{+/-}$ mice. This reduction was *Ucp1* dependent and

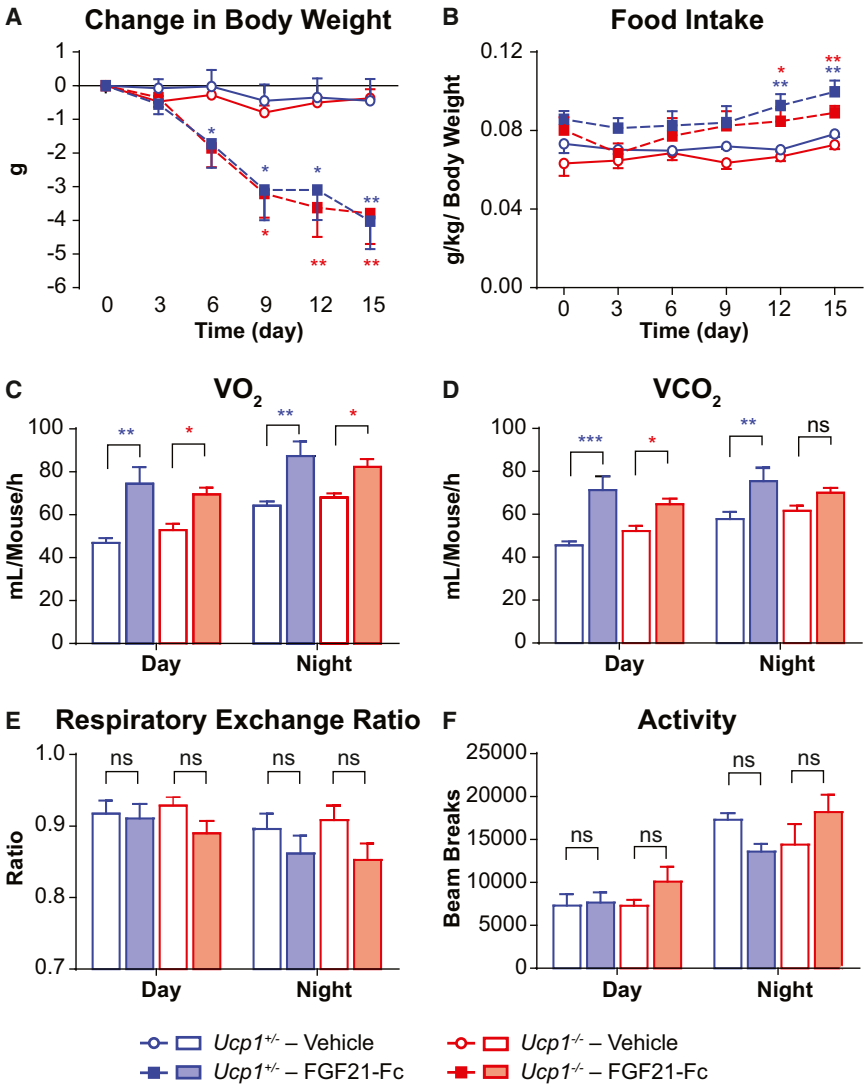

Figure 3. Increased Energy Expenditure in FGF21-Fc-Treated *Ucp1*$^{-/-}$ Mice

(A–F) *Ucp1*$^{+/-}$ and *Ucp1*$^{-/-}$ mice housed at 30°C were treated with vehicle or 3 mg/kg human FGF21-Fc per Animal Study Design II while housed in indirect calorimetry chambers. Body weight and food intake were monitored over 15 days; O_2 consumption (VO_2), CO_2 production (VCO_2), respiratory exchange ratio, and physical activity were monitored on day and night 5. Data represent mean ± SEM (n = 4 mice/group) of actual data (A and B) or whole day and night averages (C–F), analyzed by ANCOVA. *p < 0.05, **p < 0.01, ***p < 0.001 versus vehicle control of same genotype; ns, nonsignificant.

unlikely to account for any compensation of UCP1 deficiency, as it was not seen in BAT of *Ucp1*$^{-/-}$ mice. Further, the expression pattern was not repeated in iWAT. *Ucp3* expression was unaltered in BAT and iWAT of FGF21-Fc-treated mice.

FGF21 has been shown to induce the mitochondrial biogenesis regulator peroxisome proliferator-activated receptor gamma coactivator 1α (PGC-1α) (Chau et al., 2010; Potthoff et al., 2009). In our study, *Ppargc1* expression was not increased in BAT of FGF21-Fc-treated *Ucp1*$^{+/-}$ mice, consistent with previous reports (Fisher et al., 2012); however, it was significantly increased in BAT of FGF21-Fc-treated *Ucp1*$^{-/-}$ mice, suggesting possible adaptation to *Ucp1* deficiency only in the challenged state. Importantly, *Ppargc1* expression was upregulated (1.75- to 2-fold) in iWAT of FGF21-Fc-treated mice of both genotypes (Figure 4). This is consistent with other studies (Chau et al., 2010; Coskun et al., 2008; Fisher et al., 2012) and shows that PGC-1α induction, while moderate, is more coincident with FGF21-Fc-induced beneficial effects than *Ucp1* upregulation, suggesting that specifically in adipose tissue, mitochondrial biogenesis and thus mitochondrial function is related to the observed weight loss. FGF21 has been shown to increase oxidative capacity in 3T3-L1 cells, and this effect is dependent on PGC-1α (Chau et al., 2010). Our study noted increased O_2 consumption by FGF21-Fc-treated *Ucp1*$^{-/-}$ mice. In vitro data show similar increases in O_2 consumption (Chau et al., 2010), suggesting that minimal changes in *Ppargc1* expression in vivo (Figure 4) may underlie increases in O_2 consumption in *Ucp1*$^{-/-}$ mice. This effect is also consistent with a previous report identifying a relationship between FGF21 and PGC-1α in the liver (Potthoff et al., 2009), suggesting that FGF21-induced regulation of PGC-1α is a multiorgan response, potentially underlying the metabolic changes observed with FGF21 in therapeutic settings. The precise mechanism of FGF21's therapeutic effect remains unknown, although we show increased energy expenditure and higher *Ppargc1* expression that coincides with increases in body temperature, as noted by Coskun et al. (2008). This suggests that energy expenditure via increased body temperature is a potential mechanism of action and is not associated with brite in iWAT.

Our study confirms FGF21 induction of browning, but disproves the current theory that this event is responsible for its weight loss and related beneficial effects. Notably, FGF21-Fc induced significant histologic changes in lean mice at 21°C, yet these are dispensable for its beneficial effects. Thus, either FGF21-induced brite is a physiologic response for thermal defense and unrelated to the significant changes in energy expenditure that coincide with FGF21's beneficial effects, or nonshivering thermogenesis and uncoupling are parallel to mitochondrial biogenesis and activation and occur downstream of FGF21's metabolic effects. A limitation of this study is that brite activation by FGF21-Fc was assessed by histology and UCP1 presence only and not functionally. Given that cold-adapted brite mitochondria are functionally thermogenic (Shabalina et al., 2013) and dependent on UCP1 presence (Nedergaard et al., 2001), our observations likely indicate a lack of functional

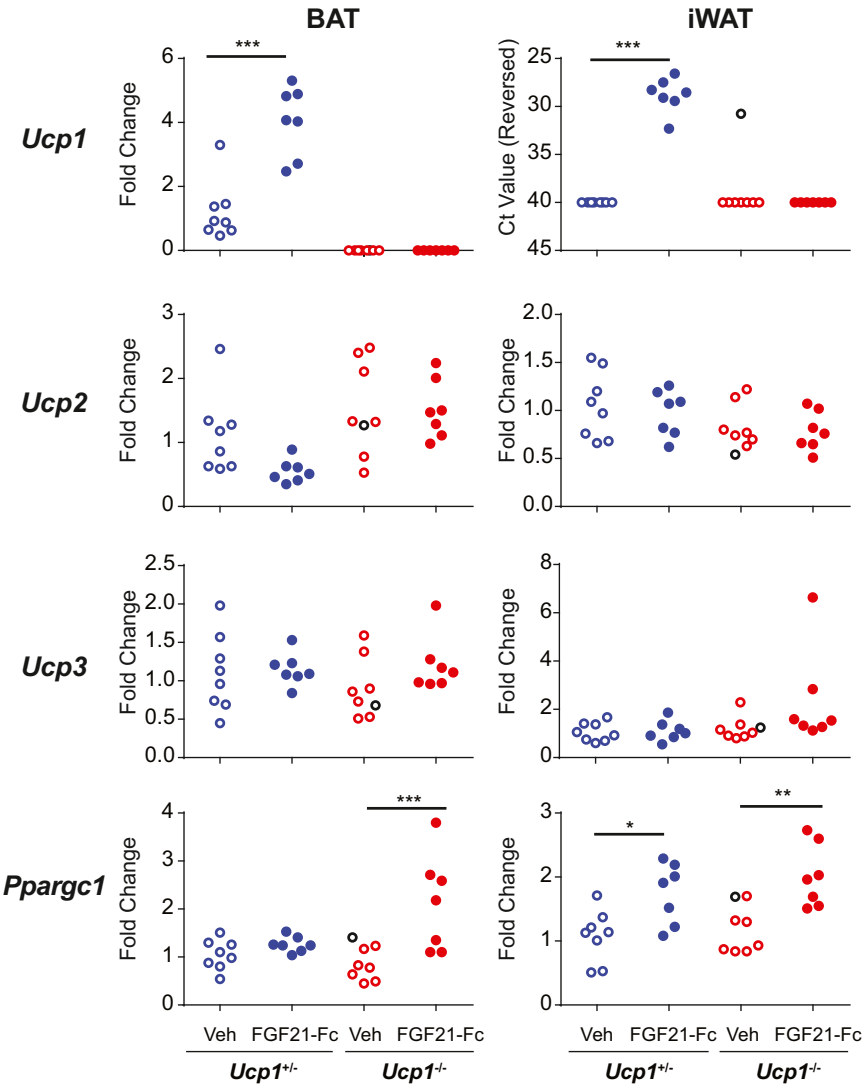

Figure 4. Gene Expression in iWAT and BAT of FGF21-Fc-Treated *Ucp1*$^{-/-}$ Mice

Fold change is expressed relative to vehicle-treated *Ucp1*$^{+/-}$ mice, except for iWAT *Ucp1* expression, which was only detected in *Ucp1*$^{+/-}$ FGF21-Fc-treated mice. Data are expressed in RT-PCR threshold cycles (Ct). An outlier based on *Ucp1* expression was identified, marked with an empty circle, and excluded from statistical analyses. Data represent individual values (n = 7–8/group), analyzed by one-way ANOVA. *$p < 0.05$, **$p < 0.01$, ***$p < 0.001$ in pairwise comparisons as indicated; only significant changes are displayed. See also Table S4.

brite in our mouse models, though this needs to be carefully tested.

In summary, only lean mice housed at 21°C showed substantial browning in iWAT post-FGF21-Fc treatment. Browning was almost absent in lean mice housed at 30°C or in DIO mice housed at 21°C or 30°C. FGF21-Fc was efficacious in *Ucp1*$^{-/-}$ mice despite UCP1 absence. Further, increased O_2 consumption was retained in FGF21-Fc-treated *Ucp1*$^{-/-}$ mice, indicating similar changes in metabolism between genotypes and environments. We propose that FGF21-induced browning in iWAT is not causative of weight loss.

EXPERIMENTAL PROCEDURES

Animal Procedures

Male mice (see Animal Design I–II for strain and genotype) were cared for in accordance with the Guide for the Care and Use of Laboratory Animals, 8th Edition. Mice were singly housed in an AAALAC-accredited facility in ventilated static housing with corn cob bedding. All research protocols were approved by the Institutional Animal Care and Use Committee. Blood samples were collected from the retro-orbital sinus of conscious mice into EDTA tubes to determine blood glucose levels (AlphaTRAK glucometer, Abbott Animal Health, Abbott Park, IL). GTT was done after intraperitoneal injection of 2 g/kg glucose in mice fasted for 6 hr. Plasma cholesterol, triglyceride, and nonesterified fatty acid (NEFA) levels were measured using the Olympus AU400e Chemistry Analyzer (Olympus America, Inc, Center Valley, PA); insulin levels were determined by ELISA (Alpco, Salem, NH). Recombinant human FGF21 and long-acting human FGF21-Fc were generated as previously described (Hecht et al., 2012).

Animal Study Design I: FGF21-Fc Treatment in Lean and DIO Mice Housed in Standard and TNZ Environments

In stage 1, 4-week-old male C57BL/6 mice (Harlan Labs, Indiana, IN) were housed at 21°C or 30°C and fed standard chow (2020X, Harlan Labs) or high-fat diets (Research Diets, D12492) for 10 or 13 weeks, respectively. Blood samples were collected before study initiation to establish baseline values for each endpoint.

In stage 2, mice were treated with vehicle or FGF21-Fc (n = 8/group). Intraperitoneal injections of vehicle, 0.5 mg/kg (DIO only) FGF21-Fc, or 3 mg/kg FGF21-Fc were administered every 3 days for 15 days. Plasma was collected on day 11 or 12 and GTT done on day 15 post-treatment initiation. At necropsy, plasma, iWAT, and BAT were collected for storage in liquid nitrogen or fixation in 10% neutral-buffered formalin.

Animal Study Design II: FGF21-Fc Treatment in *Ucp1*$^{-/-}$ Mice

Male *Ucp1*$^{+/-}$ and *Ucp1*$^{-/-}$ (Stock 3124, The Jackson Laboratory, Bar Harbor, ME) mice (age 21–27 weeks) were singly housed at 30°C and fed standard chow (2020X, Harlan Labs). Blood samples were collected before study initiation to establish baseline values for each endpoint. Mice were administered either vehicle or 3 mg/kg FGF21-Fc (n = 4–6/group) every 3 days for 15 days. Plasma was collected on day 11. GTT was done 15 days post-treatment initiation. At necropsy (day 17), plasma, iWAT, and BAT were collected for storage in liquid nitrogen. For gene expression and indirect calorimetry assessments, duplicate cohorts of mice (n = 7–8/group, gene expression; n = 4/group, indirect calorimetry) in similar age ranges received the same treatment regimen. Mice were acclimated to metabolic cages at 30°C (Columbus Instruments, Columbus, OH) before treatment initiation. Data were analyzed after 5 days of treatment.

Histopathology and UCP1 Immunohistochemistry

BAT and iWAT were fixed for 72 hr in 10% neutral-buffered formalin. All tissues were embedded in paraffin, sectioned at 5 μm, and stained with hematoxylin

and eosin (H&E). For UCP1 immunohistochemistry (IHC), the Abcam ab10983 polyclonal antibody was selected as a primary antibody after extensive screening of antibody candidates in BAT and iWAT using IHC-specific conditions. Staining specificity by ab10983 was confirmed by assessing UCP1 staining in BAT and iWAT of wild-type, as well as control *Ucp1*$^{+/-}$ and *Ucp1*$^{-/-}$ mice. After IHC protocol optimization, 5 μm iWAT sections were deparaffinized, hydrated with deionized water, and pretreated with DIVA (catalog number DV2004G1, Biocare, Concord, CA) antigen retrieval solution in a pressure cooker for 40 min. Sections were blocked with CAS block (catalog number 008120, Invitrogen, Camarillo, CA) to reduce or prevent nonspecific staining. Slides were incubated with rabbit polyclonal anti-UCP1 (catalog number ab10983, Abcam, Cambridge, MA) at 1:1,000 for 1 hr at room temperature and quenched with 3% H_2O_2. UCP1 was detected using the EnVision+ System-HRP labeled polymer anti-rabbit kit (catalog number K4003, DAKO, Carpinteria, CA) followed by visualization with DAB (catalog number K3468, DAKO). Sections were counterstained with hematoxylin. Semiquantitative grading was conducted by light microscopic evaluation of H&E and replicate UCP1 immunostained iWAT sections from all mice. Each iWAT sample was scored on a four-point grading scale based on the number of multilocular cells (singly or in aggregate) showing specific UCP1 intracellular staining (definitions and photomicrographic examples in Figure S2).

RNA Analysis

RNA was prepared using the QIAGEN RNeasy Mini Kit and analyzed with the QIAGEN RT-PCR Multiplexing system on an ABI Prism 7900 (Applied Biosystems, Foster City, CA). Oligonucleotide and probe sequences are shown in Table S4. Each reaction was carried out with 50 ng total RNA using 400 nM oligonucleotides and a 200 nM probe. Each RNA sample was run in triplicate, and *Ppia* was used as the housekeeping gene.

Immunoblot Analysis

Mechanically lysed tissues were collected in lysis buffer (catalog number FNN0021, Invitrogen) containing 1 mM phenylmethylsulfonyl fluoride and protease inhibitor (catalog number 04 693 132 001, Roche), held for 30 min on ice, and vortexed every 10 min. Lysates were then centrifuged at 500 × g for 10 min at 4°C. Equal amounts of proteins were separated by SDS-PAGE and transferred to nitrocellulose membranes. Membranes were blocked with 5% milk in 0.1% Tween-20 in PBS overnight at 4°C. Primary (UCP1, catalog number ab10983, Abcam; α/β-tubulin, catalog number 2148S, Cell Signaling) and secondary (catalog number 31460, Thermo Scientific) antibodies were incubated for 1 hr at room temperature. Specifically bound antibodies were detected using chemiluminescent substrate (catalog number 34080, Thermo Scientific).

Statistical Analyses

Analysis of covariance (ANCOVA) was performed at each time point with the baseline value as covariate if available. For gene expression analyses, a one-way analysis of variance (ANOVA) was performed with a Tukey post hoc test. The p value for pairwise comparisons is presented when the overall group effect is statistically significant ($p < 0.05$). Where only two groups of data were compared, an unpaired two-tailed t test was used. Figures display SEM.

SUPPLEMENTAL INFORMATION

Supplemental Information includes two figures and four tables and can be found with this article at http://dx.doi.org/10.1016/j.cmet.2015.04.019.

AUTHOR CONTRIBUTIONS

M.M.V., C.M., and D.J.L. designed experiments, analyzed data, and wrote manuscript. G.S., J.H., R.K., J.L., and W.F. conducted experiments, collected and analyzed data, and revised the manuscript critically for important intellectual content. All authors provided their final approval of the manuscript and agree to be accountable for all aspects of the work in ensuring that questions related to the accuracy or integrity of any part of the work are appropriately investigated and resolved.

ACKNOWLEDGMENTS

We thank Gwyneth Van and Daniel Wu for immunohistochemistry expertise and assistance, and Todd Hager for pharmacokinetic assistance. All authors are employees of Amgen Inc., with no further conflict of interest. Editorial support was provided by Shobana Ganesan, Cactus Communications, on behalf of Amgen.

Received: November 13, 2014
Revised: March 10, 2015
Accepted: April 19, 2015
Published: May 5, 2015

REFERENCES

Adams, A.C., Yang, C., Coskun, T., Cheng, C.C., Gimeno, R.E., Luo, Y., and Kharitonenkov, A. (2012). The breadth of FGF21's metabolic actions are governed by FGFR1 in adipose tissue. Mol. Metab. *2*, 31–37.

Berglund, E.D., Li, C.Y., Bina, H.A., Lynes, S.E., Michael, M.D., Shanafelt, A.B., Kharitonenkov, A., and Wasserman, D.H. (2009). Fibroblast growth factor 21 controls glycemia via regulation of hepatic glucose flux and insulin sensitivity. Endocrinology *150*, 4084–4093.

Boon, M.R., van den Berg, S.A., Wang, Y., van den Bossche, J., Karkampouna, S., Bauwens, M., De Saint-Hubert, M., van der Horst, G., Vukicevic, S., de Winther, M.P., et al. (2013). BMP7 activates brown adipose tissue and reduces diet-induced obesity only at subthermoneutrality. PLoS ONE *8*, e74083.

Chau, M.D., Gao, J., Yang, Q., Wu, Z., and Gromada, J. (2010). Fibroblast growth factor 21 regulates energy metabolism by activating the AMPK-SIRT1-PGC-1alpha pathway. Proc. Natl. Acad. Sci. USA *107*, 12553–12558.

Chechi, K., Carpentier, A.C., and Richard, D. (2013). Understanding the brown adipocyte as a contributor to energy homeostasis. Trends Endocrinol. Metab. *24*, 408–420.

Chechi, K., Nedergaard, J., and Richard, D. (2014). Brown adipose tissue as an anti-obesity tissue in humans. Obes. Rev. *15*, 92–106.

Coskun, T., Bina, H.A., Schneider, M.A., Dunbar, J.D., Hu, C.C., Chen, Y., Moller, D.E., and Kharitonenkov, A. (2008). Fibroblast growth factor 21 corrects obesity in mice. Endocrinology *149*, 6018–6027.

Emanuelli, B., Vienberg, S.G., Smyth, G., Cheng, C., Stanford, K.I., Arumugam, M., Michael, M.D., Adams, A.C., Kharitonenkov, A., and Kahn, C.R. (2014). Interplay between FGF21 and insulin action in the liver regulates metabolism. J. Clin. Invest. *124*, 515–527.

Enerbäck, S., Jacobsson, A., Simpson, E.M., Guerra, C., Yamashita, H., Harper, M.E., and Kozak, L.P. (1997). Mice lacking mitochondrial uncoupling protein are cold-sensitive but not obese. Nature *387*, 90–94.

Feldmann, H.M., Golozoubova, V., Cannon, B., and Nedergaard, J. (2009). UCP1 ablation induces obesity and abolishes diet-induced thermogenesis in mice exempt from thermal stress by living at thermoneutrality. Cell Metab. *9*, 203–209.

Fisher, F.M., Kleiner, S., Douris, N., Fox, E.C., Mepani, R.J., Verdeguer, F., Wu, J., Kharitonenkov, A., Flier, J.S., Maratos-Flier, E., and Spiegelman, B.M. (2012). FGF21 regulates PGC-1α and browning of white adipose tissues in adaptive thermogenesis. Genes Dev. *26*, 271–281.

Foltz, I.N., Hu, S., King, C., Wu, X., Yang, C., Wang, W., Weiszmann, J., Stevens, J., Chen, J.S., Nuanmanee, N., et al. (2012). Treating diabetes and obesity with an FGF21-mimetic antibody activating the betaKlotho/FGFR1c receptor complex. Sci. Transl. Med. *4*, 162ra153.

Giralt, M., and Villarroya, F. (2013). White, brown, beige/brite: different adipose cells for different functions? Endocrinology *154*, 2992–3000.

Hecht, R., Li, Y.S., Sun, J., Belouski, E., Hall, M., Hager, T., Yie, J., Wang, W., Winters, D., Smith, S., et al. (2012). Rationale-based engineering of a potent long-acting FGF21 analog for the treatment of type 2 diabetes. PLoS ONE *7*, e49345.

Hondares, E., Rosell, M., Gonzalez, F.J., Giralt, M., Iglesias, R., and Villarroya, F. (2010). Hepatic FGF21 expression is induced at birth via PPARalpha in

response to milk intake and contributes to thermogenic activation of neonatal brown fat. Cell Metab. *11*, 206–212.

Hondares, E., Iglesias, R., Giralt, A., Gonzalez, F.J., Giralt, M., Mampel, T., and Villarroya, F. (2011). Thermogenic activation induces FGF21 expression and release in brown adipose tissue. J. Biol. Chem. *286*, 12983–12990.

Hondares, E., Gallego-Escuredo, J.M., Flachs, P., Frontini, A., Cereijo, R., Goday, A., Perugini, J., Kopecky, P., Giralt, M., Cinti, S., et al. (2014). Fibroblast growth factor-21 is expressed in neonatal and pheochromocytoma-induced adult human brown adipose tissue. Metabolism *63*, 312–317.

Ito, S., Kinoshita, S., Shiraishi, N., Nakagawa, S., Sekine, S., Fujimori, T., and Nabeshima, Y.I. (2000). Molecular cloning and expression analyses of mouse betaklotho, which encodes a novel Klotho family protein. Mech. Dev. *98*, 115–119.

Kharitonenkov, A., Shiyanova, T.L., Koester, A., Ford, A.M., Micanovic, R., Galbreath, E.J., Sandusky, G.E., Hammond, L.J., Moyers, J.S., Owens, R.A., et al. (2005). FGF-21 as a novel metabolic regulator. J. Clin. Invest. *115*, 1627–1635.

Lee, P., Linderman, J.D., Smith, S., Brychta, R.J., Wang, J., Idelson, C., Perron, R.M., Werner, C.D., Phan, G.Q., Kammula, U.S., et al. (2014a). Irisin and FGF21 are cold-induced endocrine activators of brown fat function in humans. Cell Metab. *19*, 302–309.

Lee, P., Werner, C.D., Kebebew, E., and Celi, F.S. (2014b). Functional thermogenic beige adipogenesis is inducible in human neck fat. Int. J. Obes. (Lond.) *38*, 170–176.

Nedergaard, J., Golozoubova, V., Matthias, A., Asadi, A., Jacobsson, A., and Cannon, B. (2001). UCP1: the only protein able to mediate adaptive non-shivering thermogenesis and metabolic inefficiency. Biochim. Biophys. Acta *1504*, 82–106.

Potthoff, M.J., Inagaki, T., Satapati, S., Ding, X., He, T., Goetz, R., Mohammadi, M., Finck, B.N., Mangelsdorf, D.J., Kliewer, S.A., and Burgess, S.C. (2009). FGF21 induces PGC-1alpha and regulates carbohydrate and fatty acid metabolism during the adaptive starvation response. Proc. Natl. Acad. Sci. USA *106*, 10853–10858.

Sammons, M.F., and Price, D.A. (2014). Modulation of adipose tissue thermogenesis as a method for increasing energy expenditure. Bioorg. Med. Chem. Lett. *24*, 425–429.

Shabalina, I.G., Petrovic, N., de Jong, J.M., Kalinovich, A.V., Cannon, B., and Nedergaard, J. (2013). UCP1 in brite/beige adipose tissue mitochondria is functionally thermogenic. Cell Rep. *5*, 1196–1203.

Sharp, L.Z., Shinoda, K., Ohno, H., Scheel, D.W., Tomoda, E., Ruiz, L., Hu, H., Wang, L., Pavlova, Z., Gilsanz, V., and Kajimura, S. (2012). Human BAT possesses molecular signatures that resemble beige/brite cells. PLoS ONE *7*, e49452.

Véniant, M.M., Hale, C., Helmering, J., Chen, M.M., Stanislaus, S., Busby, J., Vonderfecht, S., Xu, J., and Lloyd, D.J. (2012). FGF21 promotes metabolic homeostasis via white adipose and leptin in mice. PLoS ONE *7*, e40164.

Wu, A.L., Kolumam, G., Stawicki, S., Chen, Y., Li, J., Zavala-Solorio, J., Phamluong, K., Feng, B., Li, L., Marsters, S., et al. (2011). Amelioration of type 2 diabetes by antibody-mediated activation of fibroblast growth factor receptor 1. Sci. Transl. Med. *3*, 113ra126.

Xu, J., Lloyd, D.J., Hale, C., Stanislaus, S., Chen, M., Sivits, G., Vonderfecht, S., Hecht, R., Li, Y.S., Lindberg, R.A., et al. (2009). Fibroblast growth factor 21 reverses hepatic steatosis, increases energy expenditure, and improves insulin sensitivity in diet-induced obese mice. Diabetes *58*, 250–259.